

Chapter 2

On the Role of Compliance and Geometry in Mechanical Stability of the Humans and Robots

2.1 Stability in Human-Environment Interactions

Humans demonstrate versatile and stable interactions with the uncertain environment. This is achieved through the modulation of the mechanical properties of the limb, and as a consequence, task-related restoring forces are applied in response to the environmental displacements [48–51].

Understanding the mechanisms behind the regulation of mechanical properties of the limbs in contact can provide insight into the motor control principles incorporated by the central nervous system (CNS). Such strategies thus can be potentially beneficial for the mechanical or software design of the robots, collaborating and interacting with humans.

One way to quantify the stability of the contact between the limb and the environment in postural tasks or during the movement is through the estimation of the endpoint stiffness [52]. Early studies conducted by Mussa-Ivaldi et al. [53] estimated the human arm endpoint stiffness profile by means of imposed displacements and resulting steady state force responses. Other studies analyzing the overall human arm impedance (inertia, damping and stiffness) have also been carried out [49, 54–56]. Perturbation based impedance estimation techniques are currently the most accurate and reliable, due to direct measurements of the applied force–displacement profiles. However, their application can be problematic when real-time estimation of the human arm impedance is required during the execution of the task. To that end, other studies propose more realtime techniques for the estimation of the human joint torque, or stiffness profiles [48, 57], relying on the strong correlation between task-oriented modifications of the joint torque and patterns of activations in the involved muscles [48, 58, 59]. For instance in [48], a relationship between the human arm joint stiffness and muscle activation during static force control in the horizontal plane by means of surface electromyographic (EMG) signals is established. In this study, the stiffness components of shoulder, elbow, and their cross-term and the EMG of six related muscles were measured during the tasks. Assuming that the EMG reflects the corresponding muscle stiffness, the joint stiffness was predicted from the EMG by

using a two-link six-muscle arm model and a constrained least-square error regression method. In another study [57] a mathematical muscle model based on anatomical and physiological data to estimate joint torque solely from EMG is developed. This model expresses muscle tension using a quadratic function of the muscle activation and parameters representing muscle properties. Using this model, authors were able to reconstruct joint torque from EMG signals with or without co-contraction, while the joint stiffness was directly obtained by differentiation of this model analytically.

In [60], the knee joint stiffness in isometric conditions is modeled and estimated using EMG combined with kinetic and kinematic measurements. This approach is claimed to be capable of including conditions with antagonistic muscle activation, a phenomenon commonly observed in physiological gait. Authors conclude that knee stiffness can be accurately estimated in isometric conditions using EMGs. This enables quantification of the knee stiffness during gait or similar movements of the lower body, without the need for applying perturbations.

Regardless of the technique used for the identification of the endpoint stiffness, it has been observed that its profile can be regulated in different ways. For instance, muscle activation can modify the stiffness via cocontraction of muscles involved in task execution [43], or through modifications in the sensitivity of reflex feedback [61, 62]. Former studies suggest that changes in muscle activation can appropriately change the joint stiffness (and the endpoint stiffness as a consequence), which results in increased stability and endpoint accuracy during postural tasks or movements [63–65]. Other studies report on the stiffness profile variations during more dynamic tasks. For instance in [65], it has been observed that cocontraction of the muscles increases with movement velocity and with magnitude of disturbance forces. In addition, it is proposed that higher levels of cocontraction, i.e. higher values of the endpoint stiffness profiles might be a strategy which is used by CNS early in learning a novel motor task to achieve a desired accuracy before fully learning of the dynamic models of the task.

The role of cocontraction in reduction of the kinematic variability is explored in [58]. In this study, impedance modulation is suggested as a means to suppress the effects of internal noise on movement kinematics. Simulation studies suggest that increasing the impedance through coactivation results in less kinematic variability, except for the lowest levels of co-activation, thus supporting the idea that muscular co-activation is in principle an effective strategy to meet accuracy demands.

Another way of changing the endpoint stiffness is through the change in the geometry of the limb. Due to this geometric dependence, endpoint stiffness is not uniform, but varies with the direction in which the endpoint is displaced [44]. For this reason, as an example, the arm can be less stable in certain directions than others. The postural stability can be quantitatively represented in the form of an ellipse, constructed from the eigenvalues of the endpoint stiffness matrix. The orientation of the ellipse (direction of maximum stiffness) is determined by the direction of the eigenvector associated with the maximum eigenvalue of the endpoint stiffness matrix [53]. The direction of minimum stiffness, i.e., the direction of least stability, is orthogonal to this direction. Figure 2.1 demonstrates the change in directionality

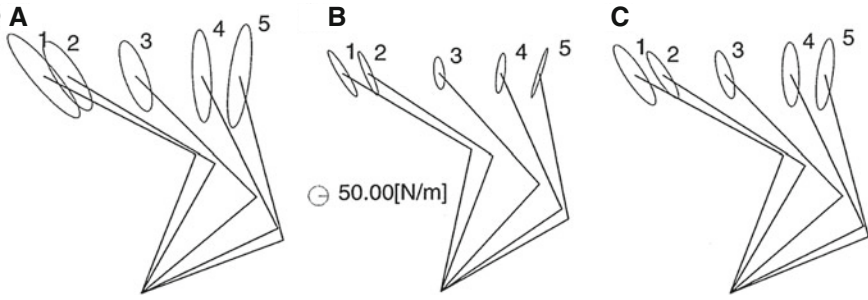


Fig. 2.1 Stiffness ellipses during posture maintenance of subjects A, B, and C

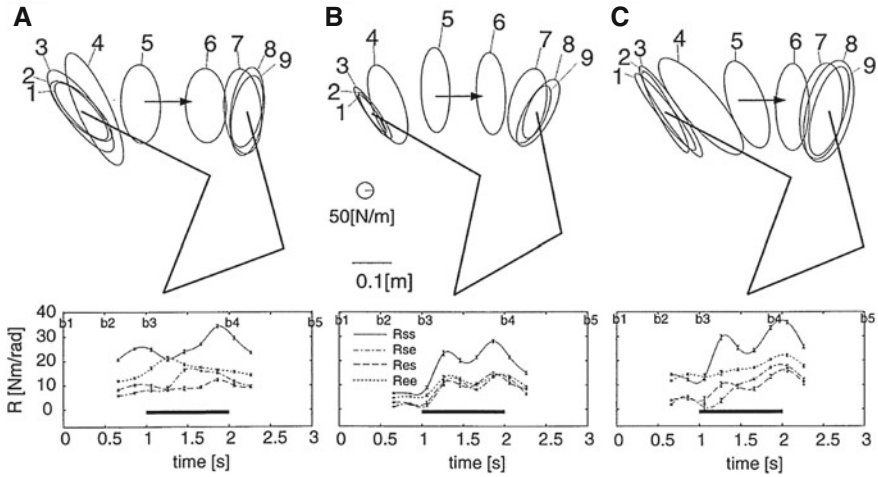


Fig. 2.2 Stiffness ellipses (*upper figures*) and joint stiffness values (*lower figures*) of shoulder (R_{ss} , *continuous curve*), elbow (R_{ee} , *dotted curve*), and double-joints (R_{se} , *dashed-dotted curve*; R_{es} , *dashed curve*) during transverse multi-joint movements for subjects A, B, and C

of the endpoint stiffness ellipsoids in static postures, where such variation during dynamic movements are depicted in Fig. 2.2. Results are inserted from [63].

If no net endpoint force is exerted by the limb, the endpoint stiffness matrix, K_C , can be related to the joint stiffness matrix, K_J , by the following equation¹

$$K_e = J^{-T} K_J J^{-1}$$

where J symbolizes the Jacobian. Above equation highlights the effect of limb geometry in realization of the endpoint stiffness matrix.

The contribution of co-activation of involved muscles in the modulation of the stiffness ellipsoid size is shown to be more effective than adjustments in its direction-

¹More detailed discussions and formulations will be provided in later chapters.

ality [44, 45]. Furthermore, previous studies discuss on limited ability of humans in changing the orientation of the postural stiffness ellipsoid, even subsequent to learning stages [66]. Instead, limb postures are adaptively regulated by the CNS to realize the desired direction of the endpoint stiffness ellipsoid. Cost efficiency of the postural adjustments compared to cocontractions and the existence of cross-joint muscles in the limbs are deemed to be the two main factors illustrating such behavior.

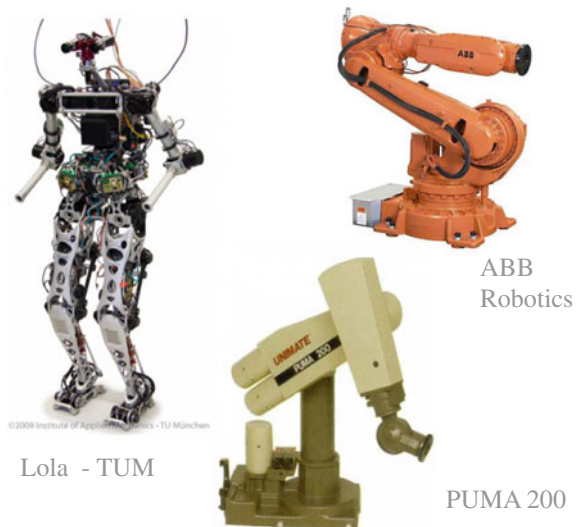
2.2 Compliant Behavior in Robots

2.2.1 Compliant Mechanisms

Replication of human-like impedance regulation mechanisms in robots can permit them to safely and efficiently operate in unstructured environments under unpredicted interaction scenarios. Previously, realization of the desired compliant behavior was extremely limited in position controlled robots (see examples in Fig. 2.3) due to the rigidity of the joints or the missing ability to command the joint torques directly. Rigidity of such robots potentially presents mechanical menaces to humans with whom robots are supposed to interact.

Over the last decades, the implementation of impedance regulation in robots is achieved by introduction of variable stiffness or torque controlled robots which can regulate actively their stiffness or full impedance properties by active/passive control techniques [67, 68]. Most of the solutions proposed have a common objective which is the reduction of the impact forces during accidental collisions between the robot and its environment or humans [69].

Fig. 2.3 Examples of position controlled robots



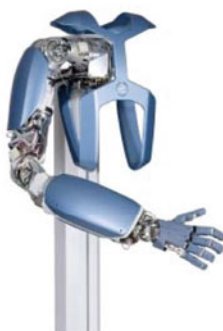
In addition to the safety, the existence of elastic elements act as storage for energy which can be fed by the kinetic energy or the gravitational potential energy of the system. This energy then can be transferred back to the system within the next cycle.

As in these types of actuators two parameters, position and stiffness have to be independently controlled; two actuators per joint are needed. One approach for implementing these joint is the use of a bio-inspired antagonistic configuration of two actuators of equal size combined with elastic elements exhibiting a nonlinear force to deflection behavior. The biological inspired joint stiffness control is a rotational joint, actuated by two series elastic actuators with nonlinear springs [70].

More recently, developments of actuation systems which inherently integrate physical principles such as variable stiffness and damping [71–74] permitted the intrinsic regulation of the robot impedance (Fig. 2.4).



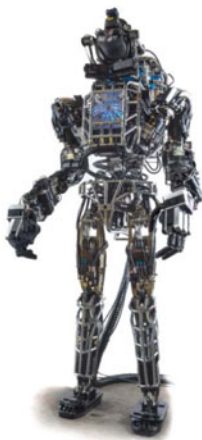
VSA CubeBot - Pisa



DLR hand-arm



COMAN - IIT

ATLAS
Boston Dynamics

Valkyrie- NASA

KUKA
Lightweight

Fig. 2.4 Recent developments in robotic systems to achieve a compliant behavior

2.2.2 Compliance Control

With the advent of higher demands on robotic manipulation, interaction with the uncertain environment using compliance control [75] became the focus of many studies in robotic systems. The contrast between this approach and the traditional position or force control methods is rooted in the context of the desired disturbance response. To establish such behavior, several techniques have been proposed [76].

Impedance control is a well known technique that establishes such desired compliant behavior by modulating the mechanical properties of the robot, while interacting with the uncertain environment. This is done by establishing a mapping from the generalized velocities to forces and is described at the tip of the end effector, i.e. Cartesian coordinates [76, 77]. Consequently, the joint motor torques of the manipulator can be calculated and tracked (see Sect. 4.1 for details).

Admittance control is another approach to achieve aforementioned desired compliant behavior. This method is implemented by controlling the manipulator in position, while the outer loop controller is in charge of rendering the compliant behavior. This is performed by measuring the generalized interaction forces at the tip of the end effector and generating the reference Cartesian trajectories. Since the algorithm incorporates position control, it has been extensively used for the compliance control of the industrial manipulators [75], as well as exoskeletons or assistive devices [78]. The main drawback of this approach is the limited ability in realizing free movements or low-impedance profiles.

In addition to above methods, there exists another approach which establishes the mapping between the Cartesian impedance profile and joint impedance values. Here, joint impedance values are being tracked by joint-level impedance controllers to realize a desired Cartesian impedance profile. Such mapping is commonly called Conservative Congruence Transformation [79].

To realize a full Cartesian stiffness matrix $K_c \in \mathbb{R}^{6 \times 6}$, the controller must track 21 independent elements of the symmetric stiffness matrix, which includes the translational, rotational, and the coupling stiffness terms. This can be achieved through control of the joint torques, impedance values and configurations [80]. Various studies address the problem of tracking the desired stiffness profile by extending aforementioned general compliance control techniques. For instance, in [81] an overview of above approaches is presented and a new controller structure is proposed, which consists of an impedance controller enhanced by local stiffness control. This structure consistently takes into account the two time scale property of the joint and Cartesian control loops. Proposed approach is experimentally evaluated in on a light weight robot. In [82], the problem of impedance control for flexible joint robots is addressed and experimentally evaluated. Combination of active impedance controller with the passive joints to further increase the stiffness range has been addressed in [83]. In this study, an algorithm to optimize the passive and active Cartesian stiffness is proposed and tested on the VSA robot DLR Hand Arm System. In [84], an admittance control scheme for a dual robot upper-limb stroke rehabilitation system is proposed.

A model of the human arm is outlined and used to formulate an admittance controller operating in human upper-limb joint space.

Even though such well-established techniques have successfully demonstrated their effectiveness through reliable handling of the contact, few studies focus on the problem of planning the variable impedance [85–88]. For instance, a comparative study of approaches for controlling robots with variable impedance actuators, in ways that imitate the behaviour of humans is presented in [86]. While, in [88], a complimentary approach is proposed which utilizes the human sensorimotor learning ability to control the robot through a multi-modal interface.

2.3 Redundancy Resolution and Its Application to Impedance Control

Redundant robots possess more degrees of freedom than are required for the basic position control of the end effector. Presence of such redundant joints can provide high versatility and dexterity to execute a certain task.

The problem of redundancy resolution was first introduced in [89], where the Jacobian pseudoinverse was utilized to solve for the motion of the redundant joints. Soon after, this problem was extensively addressed in robotics [90–94], due to the higher demands on robotic manipulation. For instance in [95], minimization of instantaneous joint torques is taken into account to resolve for the motion of the manipulator in redundant manifold. In [77], an inertia-weighted Jacobian pseudoinverse is introduced and shown to result in joint torque reduction. Incorporation of additional subtasks such as optimal joint movements [96], collision avoidance [97] or manipulator joint/torque limit avoidance [98] have also been proposed.

More general techniques incorporate an objective function, $C(q)$, of the joint angles q , and project its gradient into the manipulator Jacobian nullspace, N_J , as follows

$$\dot{q} = J^+ \dot{x} + N_J \frac{\partial C(q)}{\partial q},$$

with x denoting the end effector position/orientation vector. $[\cdot]^+$ is the pseudoinverse operator. It has been demonstrated that by using the above technique, while the desired end effector motion will be guaranteed, manipulator motions in redundant space will be regulated to stabilize a subtask variable. Such objective function can be chosen arbitrary; examples of that are gravity torque (or in general, minimum effort), manipulability, force manipulability, mechanical advantage, velocity ratio and end effector sensitivity [90].

More recent studies (e.g. see [91]), extended the above formulation for stabilization of the subtask variables in a prioritized order of occurrence. In this strategy, the desired end effector motions are usually the first priority, and others are executed in prioritized order using dynamic and kinematic redundant degrees of freedom.

Generally, redundancy resolution is performed using local or global optimum control techniques. Although the local approach is computationally inexpensive and instantaneously determines the present utilization of redundancy based on current sensory information, it lacks a guarantee of global optimality. On the other hand, the global approach is computationally costly. Thus, local approaches are the most appropriate for real time applications, where global techniques can be efficiently used for offline trajectory planning, etc.

To the author's knowledge, the problem of redundancy resolution for rendering a desired interaction performance has not been fully addressed; only few have highlighted the efficiency of the impedance control through redundancy resolution [99, 100]. For example in [99], an off line optimization technique has been utilized to realize a desired Cartesian stiffness profile in passively compliant, uncoupled joints. In [100], the issue of low stiffness in machining tasks is addressed with an integrated offline planner and real time replanner. The available manipulator stiffness is maximized during offline planning through a trajectory resolution method that exploits the nullspace of the robot machining system. In response to unmodeled disturbances, a real time trajectory replanner utilizes a time scaling method to reduce the tool speed, thereby reducing the demand on the actuator torques, increasing the robot's dynamic stiffness capabilities. During real time replanning, priorities are assigned to conflicting performance criteria such as stiffness, collision avoidance, and joint limits.

In this book, relying on the major contribution of the arm configuration to effective regulations of the endpoint stiffness ellipsoid direction, and its low-cost nature [44, 45, 66, 99, 100], we explore the role of *configuration dependent stiffness* (CDS) control, for single (Chap. 5) and dual-arm (Chap. 6) object manipulation. We propose a real time optimization technique for control of the joint variables in redundant space to realize a task-specific Cartesian stiffness matrix.

Transferring Human Impedance Regulation Skills to
Robots

Ajoudani, A.

2016, XXIV, 167 p. 85 illus., 76 illus. in color., Hardcover

ISBN: 978-3-319-24203-3